

A Comprehensive Approach to High-Resolution Daylight Imaging for SSA

Michael Hart,^{1,3} Stuart Jefferies,^{2,3} Douglas Hope,⁴ James Nagy,⁵ and Ryan Swindle⁶

¹College of Optical Sciences, University of Arizona, 1630 E. University Blvd., Tucson, AZ 85721

²Dept. of Physics and Astronomy, Georgia State University, Atlanta, GA 30303

³Institute for Astronomy, University of Hawaii, 34 Ohia Ku Street, Pukalani, HI 96768

⁴US Air Force Academy, Dept. of Physics, 2354 Fairchild Dr., Colorado Springs, CO 80840

⁵Dept. of Mathematics and Computer Science, Emory University, Atlanta, GA 30322

⁶AFRL/RD, 550 Lipoa Parkway, Kihei, HI 96753

ABSTRACT

High resolution daytime imaging of resident space objects (RSO) from the ground is presently severely challenging. At visible wavelengths, where diffraction-limited resolution is the highest before the atmosphere becomes opaque in the UV, shot noise from the bright background degrades the information that may be recovered from RSO imagery. Total exposure times must be limited in order to avoid motion blur induced either by the object's intrinsic rotation or simply by its orbital motion over the site. Fundamentally, then, one cannot collect enough light from the object to achieve adequate signal-to-noise ratio (SNR) in the presence of very high noise before the apparent shape of the object has changed. To overcome this limitation, we propose in this paper a suite of techniques which we believe will collectively enable high-resolution imaging during daylight. The approach, which has yet to be fully implemented, relies on a sequence of short-exposure images from a high-cadence camera together with simultaneous wave-front sensor (WFS) measurements acquired from a filtered sodium laser guide star. We then directly estimate the three-dimensional shape of the RSO using a formalism similar to the concept of deconvolution from wave-front sensing (DWFS). In this way, provided that the intrinsic shape of the RSO does not significantly change during the course of the observations, we can combine data from quite different pose angles in order to achieve a high-resolution result with adequate SNR. By adopting this approach, we expect an improvement of 3-4 stellar magnitudes in the faintest satellites that may be characterized independent of the telescope and observing waveband. Furthermore, a model derived from observations by one sensor may be used as the basis for the restoration of data sets from widely disparate telescopes and sensor modalities; data fusion in this sense is a natural feature of the approach.

1. MOTIVATION

The capabilities of ground-based EO/IR telescopes supporting Space Situational Awareness (SSA) are presently severely restricted during the day. Photon noise from the bright sky background obscures the signal from resident space objects (RSO). Furthermore, high-resolution observations supported by wave-front sensor (WFS) measurements either through adaptive optics (AO) or numerical post-processing are hampered by low signal-to-noise ratio (SNR) and saturation of the WFS.

The problem is particularly severe for LEO objects: their proximity to the Earth means that, even at night, they are observable only around dawn and dusk. In addition, SSA observations are very challenging for an important class of sun-synchronous orbits which only appear over a given site during the day and are presently hard to image at all. The lack of access to round-the-clock observation has unfortunate consequences for space surveillance by limiting the efficiency of sensors in collecting data of both tactical and strategic importance.

Daytime sky surface brightness is typically $m_V = 4-5$ magnitudes per sq. arcsec. To give a specific example, at the 3.6 m AEOS telescope on Mt. Haleakala this corresponds to approximately 5×10^5 photon/ms/arcsec² in the I band. In the short exposures needed by high-resolution imaging systems to freeze the atmospheric aberration, a faint satellite blurred by seeing to 1 arcsec must therefore be as bright as $m_V = 9$ simply to be detected with an adequate SNR of 10. High resolution image restoration to support object characterization, the focus of this paper, imposes a much more stringent requirement: SNR = 10 *per resolution element of the telescope*. The only way to achieve adequate SNR in the presence of the high background photon noise as the object becomes fainter is to accumulate signal over longer periods. This is a fundamental physical limitation, and Nature is not kind: the SNR for background-limited observations improves only as the square root of the integration time.

In daylight conditions, AO compensation and a direct long integration on the imaging camera is very difficult for objects that are too faint to offer a reference for tip-tilt sensing. This challenges even those AO systems which rely on one or more laser guide stars (LGS) to provide the wave front information since tip-tilt is not measurable from the LGS signals either. On the other hand, numerical restoration from sequences of short exposures remains feasible. The fundamental difference is that in the case of AO, if the tip-tilt compensation is incorrect, the RSO image is irretrievably blurred by image motion whereas post-processing, relying on sequences of short exposures, can take the time to find the optimal image centration. Our work, and this paper, therefore focus on techniques to enable numerical restoration as a means to recover high-resolution imagery.

2. NECESSITY FOR 3D OBJECT RESTORATION

Numerical object restoration relies on sequences of short exposures, each of which is on the order of the atmospheric coherence time τ_0 . By restricting the exposure time, high spatial frequency information about the object, encoded in the speckle structure of the image, is preserved. At the extreme faint end of the object brightness distribution, which we define as $\text{SNR} \ll 1$ for exposures equal to τ_0 , objects become buried in the shot noise of the sky background. To achieve adequate SNR for characterization in these circumstances, total data collection time across the entire image sequence must therefore be so long that the object's appearance in the telescope's focal plane cannot be assumed to be constant either because of its intrinsic rotation or because of its orbital motion over the site. Hence existing 2D image restoration approaches, e.g. multi-frame blind deconvolution (MFBD) and deconvolution from wave-front sensing (DWFS) [1], fundamentally cannot succeed. Instead, we propose that a solution may be found based on the observation that although the view of the object as seen by the telescope changes, and possibly also its illumination, on the time scale of the data collection the *object itself* does not.

Removing the atmospheric blur requires a high quality wave-front estimate. Even though we consider the case where, by hypothesis, the object itself is too faint for wave-front sensing, a sodium LGS may be used for the purpose during full daylight by placing a narrow-band atomic vapor filter ahead of the WFS to block the sky background. A companion paper in these proceedings by Jefferies et al. [2] describes our experimental evidence for the daylight use of sodium LGS, as well as new theoretical analysis showing how focus anisoplanatism in the LGS measurements may be mitigated by tomography [3]. We propose the use only of a single LGS, yet we show that tomography is enabled by short-term temporal coherence of the wave front for observations of earth-orbiting objects.

The limited performance that may be expected from restorations of daytime data using present methods is illustrated in Fig. 1. Here we show results obtained with the Daylight Object Restoration Algorithm (DORA) [4] from simulated observations of SEASAT under conditions of full daylight sky illumination, modeling a solar phase angle of 40° . DORA relies on short-exposure image sequences and simultaneous WFS measurements to derive an initial object and point-spread function (PSF) estimates, followed by a joint estimation step to iteratively improve the estimates until convergence. In this instance, two cases were run, where we have assumed a problem in which the changing satellite pose allows 8 frames of data to be restored before the object can no longer be considered constant.

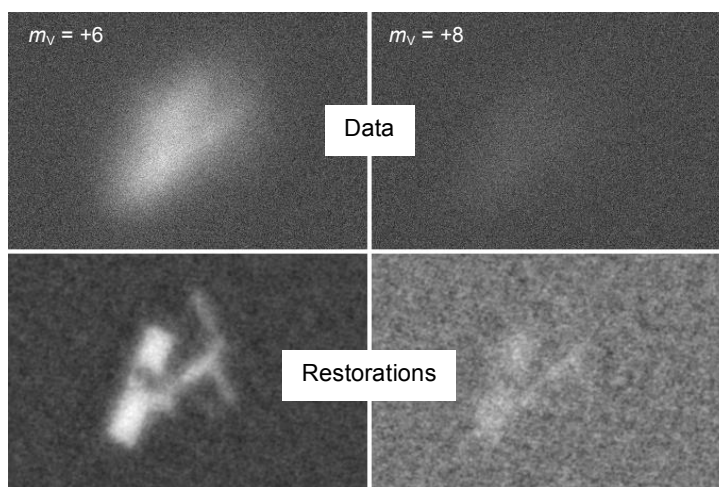


Fig. 1. Simulated data and DORA restorations of daylight imagery at $D/r_0=40$ and $0.85 \mu\text{m}$ wavelength.

The satellite was taken to be faint, with photon noise equivalent to integrated magnitudes of 6 and 8. No detector read noise was included, but would in any case be well below the shot noise from the background.

The restoration at $m_v = 8$ does show some features of the satellite, yet the fidelity of the restoration and its intelligence value are limited by the SNR of the data, attributable ultimately to the inability of the algorithm to cope with changes in the orientation of the object. To achieve better results, a longer data set is needed, and the formalism to address the 3D nature of the object.

3. OBJECT RECONSTRUCTION APPROACH

Our extension to the DORA approach, which we call DORA-3D, fuses the mathematical formalism of image restoration to remove blur [1,5] with the formalism of tomographic projection matching to recover 3D structure [6,7]. Both are individually non-linear optimization problems. The requirement is to establish a single joint mechanism to find the non-linear least-squares solution in which the 3D structure, the object's orientation and illumination parameters, and the PSFs in the data images are treated as the variables to be estimated.

The challenge is twofold: first, an appropriate formulation of the problem must be written down as a function F explicitly describing the dependence on the estimation variables of each pixel intensity I observed in the images:

$$I(\xi, \nu, t) = F\left[O(x, y, z, \lambda); \Theta(t); P(x, y, t, \lambda)\right]. \quad (1)$$

Here, O is the object brightness distribution, P is the instantaneous PSF, and Θ is a vector of five parameters specifying the observing geometry. Three of these are constant throughout the entire data set: the intrinsic rotation rates of the object about the three spatial axes. The remaining two parameters specify the position of the object in each frame. Coordinates (ξ, ν) represent a point in the focal plane, (x, y, z) represents a point in object space, and t and λ are time and wavelength. We assume that parameters related to the orbit of the object, including its range as a function of time, are known in order to allow the object to be tracked in the first place.

Second, we seek an appropriate optimization approach to minimize the mean-square residual

$$\varepsilon = \left\langle (I - I_d)^2 \right\rangle \quad (2)$$

where I_d are the data values and the angle brackets are the ensemble average over the entire data set. From Eq. 1 we calculate the analytic derivatives of Eq. 2 with respect to each of the estimation variables, and iteratively adjust the variables until ε is minimized. We anticipate that full joint optimization of all variables will offer the most robust solution, but such an approach is almost certain to be computationally infeasible. Other algorithms such as alternating direction method of multipliers (ADMM) which reduce the problem complexity by breaking it into smaller pieces and are more computationally tractable are likely to yield reasonable solutions in a small fraction of the computer time. While other fit-to-data terms for the optimization besides least-squares could be considered, the problem formulation is already sufficiently complex that we believe it will be helpful to keep this part simple. In addition, the least squares approach has been very successful in realistic imaging situations [4]. Additional regularization terms will need to be included with the objective function of Eq. 2 in order to arrive at solutions robust to the high level of noise in the problem; various techniques may be considered, including iteration truncation, Tikhonov, and total variation.

In posing the problem we assume that the viewing and solar illumination geometry is known. This allows any 2D projection (i.e. image) to be calculated from the evolving 3D model according to a specified viewing angle, including the effects of self-shadowing, and allows analytic derivatives of Eq. 2 to be calculated.

The object is modeled in a 3D voxel grid using an approach first developed by us for automatic target recognition applications [8]. The object variables to be estimated at each grid point are the brightness, normal vector, and the opacity. We know that, at convergence, the opacity will be either 0 (transparent) or 1 (opaque), where the opaque voxels define the location of the satellite hull. To begin, however, we assume that we know nothing about the shape of the hull, and so all the opacities are set to a uniform value $0 < \nu < 1$ such that the integral along any line of sight through the model is unity. We treat the brightness in the same way. This reflects our maximum ignorance. In this sense, the opacity may be thought of as a probability density function, reflecting the present state of our knowledge of the location of the hull. Proceeding, projected views are calculated corresponding to each data frame's known geometry, taking into account the real-valued opacities. The views are convolved with the corresponding PSFs derived from the LGS WFS to arrive at the data models I which are to be compared directly to the data I_d to

calculate the cost function in Eq. 2. Our candidate optimization algorithms are then employed to iterate on the opacity and brightness variables, as well as the PSF and satellite pose variables, to bring the data model and the data into agreement. In this way, we use all the data to derive a single 3D object estimate in a self-consistent manner.

An illustration of 3D estimation using a stereoscopic code is shown in Fig. 2. Here, two uncompensated five-frame image sequences of the Hubble Space Telescope (HST) recorded by the AEOS 3.6 m telescope have been restored using DORA. The data frames present HST at pose angles separated by about 7° . For the parts of the object that can be seen in both frames this is sufficient to establish a 3D model comprising brightness and normal vectors at each voxel. The lower panels of Fig. 2 show a sequence of images of HST synthesized from the 3D model at 1° increments.

This result was obtained using a serial processing sequence of object restoration followed by standard stereoscopic 3D estimation. In the DORA-3D implementation, these steps will be carried out jointly, using all the available data

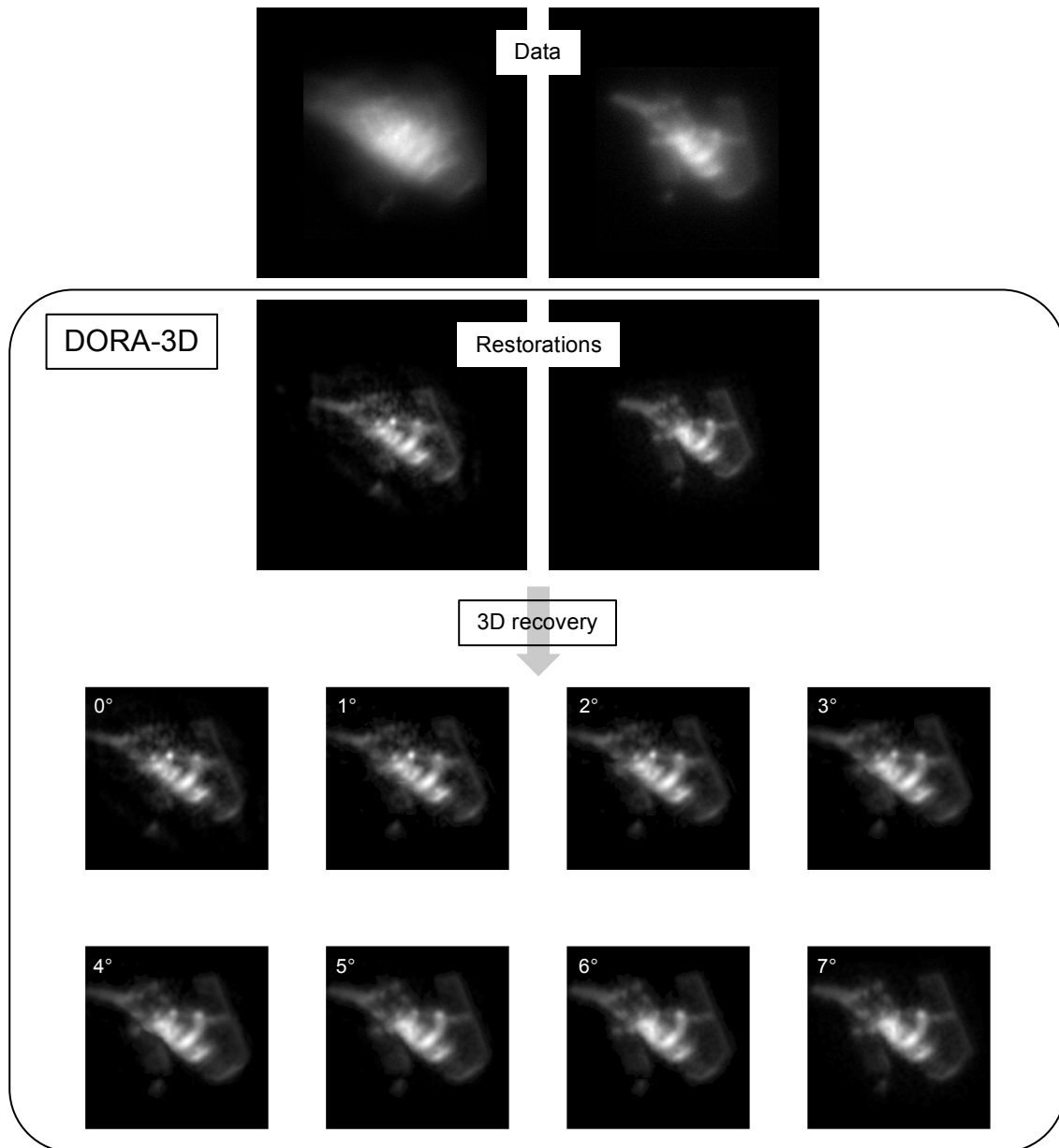


Fig. 2. (Top) Raw data frames of HST from the AEOS telescope. (Middle) Restored objects. (Bottom) Progression of views derived from a 3D model constructed from the restored images.

frames rather than just two. The model in Fig. 2 is limited because not all parts of HST are observable in the two data frames; synthesized images would become increasingly inaccurate as the point of view departed from the range of pose angles spanned by the data. This will generally be true as well of more realistic data sets with many thousands of frames. However, a partial model developed with one data set may serve to initialize the restoration of another, and in turn be refined and expanded to cover additional parts of the satellite.

Because of the limited data, the voxels of the 3D model computed from HST had the same spatial extent as the pixels in the images. Joint 3D estimation however will need to be computed on a denser grid to support higher resolution enabled by subsampling of object structure by the movement of pixel boundaries across many frames.

4. KEY CHALLENGES

The approach presents a major technical challenge overall, in the first instance because we are looking to characterize objects that are essentially invisible in the raw data. There are also several hurdles to be overcome because of the sheer number of variables that must be estimated: we will require on the order of 60 s of data recorded at roughly 1000 frames per second. Each data frame may be expected to be $\sim 256 \times 256$ pixels, and a PSF of this size must be estimated for each frame. The object will initially be estimated in a $256 \times 256 \times 256$ cube. By comparison, the remaining variables (pose estimation) are negligibly few, but overall, this leads to roughly 10^{10} variables.

An estimation problem on this scale requires a very efficient implementation of the solver, and quite possibly novel methods to scan and/or constrain the search space to identify the region containing the global minimum of the objective function. An additional challenge is posed by the discontinuous derivatives of Eq. 2 that will arise because of self-shadowing by re-entrant components of the satellite. This may require a partial computation of the Hessian matrix to identify areas of the data where this is happening, and careful treatment of those regions by the solver.

5. VALUE TO SSA

By adopting the approach proposed in this paper, SSA telescopes will be able to collect data continuously during the day, which for LEO objects is now possible only during ~ 1.5 hour periods near dawn and dusk. While pointing directly at the sun will still need to be avoided, a roughly $5 \times$ improvement in overall data collection availability for such objects will be realized. In addition, SSA observations will be enabled for an important class of sun-synchronous orbits which only appear over a given site during the day and are presently very hard to image at all. Furthermore, spatio-spectral characterization will be possible for satellites that are presently well below the brightness limit even for detection during the day. Independent of the telescope and waveband, characterization will be achieved on satellites 3-4 stellar magnitudes fainter for a typical LEO object than is currently possible.

The utility of our proposed approach, however, goes well beyond making high-resolution snapshots for evaluation by human analysts. The 3D model itself, derived initially from a single pass over a single sensor, represents our state of knowledge of that particular satellite. The model can then serve as the starting point in the restoration of data from successive passes, even if the viewing geometry is quite different, and on every pass, the model can be refined. In fact, it will be important to build the model on a voxel grid rather finer than the pixel scale of the imaging camera because dithering of small features across pixel boundaries in multiple data sets will allow interpolation on spatial scales smaller than the Nyquist limit of the camera. Furthermore, once the model has reached a reasonable degree of fidelity, change detection on further passes becomes feasible, for instance to assess satellite health or activity: the movement of solar panels, articulations, or antennae.

Looking further, with the 3D framework in place, the model may be extended to include other variables associated with each voxel, for example spectral signatures, material composition, polarization, or radar cross-section when such data are available. Similarly, the same model may be used as the basis for the restoration of data sets from widely disparate telescopes and sensor modalities; data fusion in this sense is a natural feature of the approach. In this way, for example, a model developed with data from a 1 m telescope could be used to directly constrain the restoration and interpretation of data from a 3.5 m telescope, effectively acting as prior information. Furthermore, although we anticipate that the method will find its greatest value in addressing the extreme faintness limit in the EO/IR bands, we note that the mathematical approach is by no means confined to that regime. More traditional observations where wave-front sensing relies on the object itself, such as those now made at the AEOS 3.6 m and the SOR 3.5 m telescopes, will be perfectly suited to analysis in the same way.

6. CONCLUDING REMARKS

Adopting a common sensor-agnostic multi-dimensional object model across data modalities and sensor locations will potentially increase the efficiency of a wide range of existing surveillance assets presently supporting the space object catalog. This extends to non-resolved measurements from ongoing programs and data supplied by commercial companies: for example, light curve fluctuations should be consistent with the models. In this sense, an object model can serve as an unbiased consistency check across all modalities: contributing sensors that continually produce data in line with the model predictions would be ranked as more trustworthy than those that do not. The approach has the potential therefore to set a new community-wide paradigm for the synthesis and interpretation of SSA observations.

7. REFERENCES

1. Jefferies, S. M. and Hart, M., “Deconvolution from wave-front sensing using the frozen flow hypothesis,” *Opt. Exp.* **19**, 1975–1984 (2011).
2. Jefferies, S. M., Hart, M., Hope, D. A., and Murphy, N., “Daylight operation of a sodium laser guide star for wave front sensing,” *Proc. AMOS Tech. Conf.* (2016).
3. Hart, M., Jefferies, S. M., and Hope, D. A., “Atmospheric tomography for artificial satellite observations with a single guide star,” *Opt. Lett.* **41**, 3723–3726 (2016).
4. Hope, D. A., Hart, M., Jefferies, S. M., and Nagy, J. G., “Robust image restoration for ground-based space surveillance,” *Proc. AMOS Tech. Conf.*, E51, (2013).
5. Jefferies, S. M., Hope, D. A., Hart, M., and Nagy, J. G., “High-resolution imaging through strong atmospheric turbulence,” *Proc. SPIE* **8890**, 88901C (2013).
6. Chung, J., Sternberg, P., and Yang, C., “High-performance three-dimensional image reconstruction for molecular structure determination,” *IJHPCA* **24**, 117–135 (2010).
7. Penczek, P., Radermacher, M., and Frank, J., “Three-dimensional reconstruction of single particles embedded in ice,” *Ultramicroscopy* **40**, 33–53 (1992).
8. Overman, T. L. and Hart, M., “Sensor agnostic object recognition using a map seeking circuit,” *Proc. SPIE* **8391**, 83910N (2012).